LAWRENCE
LIVERMORE
NATIONAL
LABORATORY

UCRL-CONF-223845

Active Detection of Small Quantities of Shielded Highly-Enriched Uranium Using Low-Dose 60-keV Neutron Interrogation

P. Kerr, M. Rowland, D. Dietrich, W. Stoeffl, B. Wheeler, L. Nakae, D. Howard, C. Hagmann, J. Newby, R. Porter

August 21, 2006

Conference on the Application of Accelerators in Research and Industry
Fort Worth, TX, United States
August 21, 2006 through August 25, 2006

Active Detection of Small Quantities of Shielded Highly-Enriched Uranium Using Low-Dose 60-keV Neutron Interrogation

Phil Kerr[1], Mark Rowland[1], Dan Dietrich[1], Wolfgang Stoeffl[1], Boyd Wheeler[1], Les Nakae[1], Doug Howard[1], Chris Hagmann[1], Jason Newby[1], Robert Porter[2]
[1]Lawrence Livermore National Laboratory, Livermore, CA 94550
[2]California Polytechnic University, San Luis Obispo, CA 93407

Abstract
Active interrogation with low-energy neutrons provides a search technique for shielded highly-enriched uranium. We describe the technique and show initial results using a low-dose 60 keV neutron beam. This technique produces a clear induced fission signal in the presence of small quantities of ^{235}U. The technique has been validated with low-Z and high-Z shielding materials. The technique uses a forward-directed beam of 60 keV neutrons to induce fission in ^{235}U. The induced fission produces fast neutrons which are then detected as the signature for ^{235}U. The beam of neutrons is generated with a 1.93 MeV proton beam impinging on a natural lithium target. The proton beam is produced by a radio-frequency quadrupole (RFQ) LINAC. The 60 keV neutron beam is forward directed because the ^{7}Li(p,n) reaction is just at threshold for the proton energy of 1.93 MeV.

PACS Codes: 25.85.Ec, 29.40.Mc, 29.47.-n, 89.20.Bb
Keywords: active neutron interrogation, pulse-shape discrimination, neutron-induced fission, non-destructive assay

Introduction
Detection of small quantities of shielded highly-enriched uranium (HEU) is possible using a low-dose, low-energy, active neutron interrogation technique. This technique is being applied to the problem of detection of illicit HEU in cargo. The technique uses a portable radio-frequency quadrupole (RFQ) proton LINAC to produce a forward directed 60-keV neutron beam. The 1.93 MeV proton beam strikes a ^{7}Li target just above threshold for the ^{7}Li(p,n) reaction, producing a forward directed beam with average energy of 60-keV. The 60-keV neutron beam induces fission ^{235}U which then emits a spectrum of fission neutrons. The highest energy neutrons (>500keV) are detected with a neutron and gamma-ray pulse-shape discriminating (PSD) scintillator detector.

The neutron data is most informative in a two-dimensional histogram of detector pulse fall time versus pulse height. In a one-dimensional projection onto the time axis, this produces the familiar double peak spectrum from pulse-shape discrimination of gamma-rays and neutrons. Figure 1 shows one such two-dimensional plot obtained during active interrogation of 80g of ^{235}U. This was the ^{235}U content in a 39 kg sample of depleted uranium. There is a very strong high-energy neutron band in the plot due to induced fission. Figure 2 shows an equivalent mass of non-^{235}U containing material interrogated with 60-keV neutrons. In this case, there is virtually no neutron signal. Figure 3 shows the experimental layout.

The fast neutron signal occurs synchronous with the interrogating beam. This requires a detection system capable of ignoring the interrogating 60 keV beam while at the same time

detecting the induced fission neutrons from ^{235}U. The fast neutron fission signal is detected with pulse-shape discriminating scintillators, calibrated to ignore the low-energy interrogating beam and the gamma-rays from background and other sources. Particle identification and energy thresholds can be set in the spectrum to count only high-energy fission neutrons produced when the low-energy neutron beam induces fission in ^{235}U that is present. The technique therefore allows a direct detection of the ^{235}U signature even while the 60 keV neutron beam is on. In addition, the technique reduces by many orders of magnitude the neutron dose required for detection compared to techniques using delayed gamma-ray signatures from active neutron interrogation. In addition, the 60 keV neutrons do not appreciably fission ^{238}U or ^{232}Th. This is because at 60 keV, the fission cross section is more than four orders of magnitude lower than that for ^{235}U, as seen in Figure 4.

We mention two issues of comparison of 60 keV interrogation to interrogation with high energy neutrons: penetration and dose. In any active interrogation scheme, neutrons must find their way into the target, possibly through various shielding materials. The 60 keV neutrons penetrate nearly as deeply as high energy neutrons. This is because the high energy neutrons slow down by nuclear excitation (n, n') reactions as well as inelastic scattering, while the 60 keV neutrons slow down only by inelastic scattering. The high-energy neutrons have some penetration advantage in hydrogenous material, roughly by the first mean free path since elastic scattering cross sections are smaller for high energy. (This smaller scattering cross section enables the fast fission neutrons created to get out.)

In non-hydrogenous cargo the thermalization path length is approximately 50 meters. If special nuclear material (SNM) is hidden in such cargo, the 60 keV neutrons will usually diffuse until they induce fission rather than being lost to capture. Table 1 shows simulation results comparing, for different neutron sources, the number of fissions induced in HEU per source neutron. A 5 kg ball of HEU (4 cm radius) is in a shipping container (2.5 x 2.5 x 6 m^3). The container wall is 0.5 cm iron. The container is sitting on a 20 cm thick concrete floor, and filled uniformly to a density of 0.4 g/cm^3 with different materials as listed in Table 1. The neutron source is 2 m from the uranium ball. The 60 keV neutrons give less neutron radiation dose per neutron than high energy neutrons. As shown in Figure 5, the direct biological dose from 60 keV neutrons is 40 times lower than for 14 MeV.

High energy neutrons also create additional neutron activation due to induced nuclear reactions like (n, 2n). As for any active interrogation, there is a dose from neutron capture gamma-rays. Also, despite the forward beaming of the 60 keV beam, some neutron flux will backscatter. The amount of backscatter and capture gamma-rays is configuration dependent, but will be less than for high-energy neutron interrogation. Because essentially every induced fission produces fast-neutrons, the strength of our interrogator probe for a scaled system is about 10^8 neutrons per second. This much less than for detection schemes based on a signal from fission fragment decays from only a fraction of the induced fissions.

The observation of high-energy neutron emission while interrogating with low energy neutrons is a powerful and direct signature of special nuclear materials. The technique is less effective for hydrogenous cargo and the limits in this regard are still being investigated. However, a fast-neutron signal has been detected from hydrogenous overburdens such as polyethylene and

plywood as described below. Here we present experimental data to demonstrate the technique, as well as descriptions of the RFQ, detectors, and data-acquisition system.

Neutron Generator

An RFQ is well suited to accelerate ions in the velocity range from 0.01c to 0.1c, where c is the speed of light. The RFQ is, however, not suitable to accelerate electrons. The one-meter section of RFQ in the present portable neutron generator can accelerate protons to 2 MeV. The four electrodes of the RFQ (see Figure 6) are excited with quadrupole mode RF voltages to focus the beam. The electrodes are also modulated by the RF to produce longitudinal electric fields that accelerate low-velocity ions to high energy.

The fully assembled RFQ 60-keV neutron generator is shown in Figure 7. The unit can be easily disassembled into a top and bottom half. The two halves are connected by five cables, including the large 150 kW RF power cable. The top half weighs 240 lbs and contains the RFQ cavity, ion source, target assembly, vacuum systems, small hydrogen bottle, and control panel. The bottom half weighs 250 lbs and contains the compact 150 kW, 600 MHz solid state RF generator, the high voltage supply, and the capacitor bank. All components are air-cushion shock mounted to survive rough handling. All LINAC and RF functions are controlled from a compact control panel on top of the LINAC.

A drive loop antenna is used to couple 150 kW of 600 MHz RF into the RFQ cavity. The four vane tips produce a 70 kV p-p gradient and a net forward propulsion for the protons. The power comes from a compact 150 kW, 600 MHz solid state RF generator. The maximum duty cycle is 1%. The RFQ is run at a duty cycle of 0.5%. The whole LINAC system is mounted in two portable boxes and draws 2 kW AC power at 220V.

Ion Source

The portable 60-keV neutron generator uses a 2.5 GHz proton ECR source. The plasma is excited by 200 Watt of 2.5 GHz RF power. The source antenna is shaped to match the resonance of the 2.34 GHz amplifier peak power. A 21 kV Einzel Lens and extractor cone serves to pre-accelerate and focus the proton beam into the RFQ LINAC.

The very small source is capable of producing 6 mA of proton current through the Einzel lens, and 0.8 mA of protons through the LINAC. The maximum 60 keV neutron flux in the forward direction is reached when the proton energy is about 1.91 MeV. If the proton energy is higher, most of the neutrons are emitted sideways and backward.

Target

The ^{7}Li target consists of a 2 mm silver disk coated with the following materials:

- 10 micro-meter natural lithium (75 keV loss)
- 120 nm chromium (8 keV loss)
- 110 nm aluminum (3 keV loss)

A quadrupole permanent magnet expands the beam enough so that the lithium target does not melt. Close to threshold, all neutrons are emitted in the forward direction for kinematic reasons. Figure 8 shows the calculated energy and angle neutron distribution for an incident proton

energy of 1.93 MeV. An examination of Figure 8 shows that the beam is forward peaked. The energy in the forward direction is most intense at about 60 keV +/- 30 keV. Some of the neutrons, though, have energies that range from as high as 140 keV, and down to thermal on the low energy side. Away from the forward direction, the energy spectrum softens. By 90°, the beam intensity has dropped to less than 10% of the forward intensity and the energy spectrum is below 10 keV.

Fast Neutron Detection

In addition to the induced fission neutrons and the presence of normal background gamma rays, active neutron interrogation produces gamma rays when 60-keV neutrons are captured in surrounding materials and a capture gamma rays are emitted. The 60 keV neutron active interrogation technique relies on detectors that are able to distinctly count the induced high-energy fission neutrons in the presence of the 60-keV neutron interrogation beam and background gamma-rays. The most effective neutron detection materials which satisfy this requirement are scintillators with neutron and gamma-ray pulse-shape discrimination (PSD) properties. The most common of these types of detector are the xylene-based liquid scintillator and stilbene crystal ($C_{14}H_{12}$). These materials are sensitive to neutrons through proton recoils producing scintillation light. They are sensitive to gamma rays through Compton scattered electrons producing scintillation light. A photomultiplier tube (PMT) is attached to the scintillator to convert the scintillator light signal to a measurable electronic pulse. Liquid scintillators have a 78% intrinsic detection efficiency for 1 MeV neutrons. Discrimination against gamma rays with liquid scintillators using PSD is about 10 times better than for plastic scintillators[1].

The fission neutron detection for this work was done with a single 3” x 3” liquid scintillator detector connected to a neutron/gamma-ray pulse-shape discrimination (PSD) system. The familiar NE-213 xylene-based liquid scintillator is now available from Bicron as BC-501A and from Eljen Technology as EJ-301. Xylene is the bulk solvent aromatic host material. Into this solvent is dissolved a proprietary type and amount (usually ~0.5%) of a fluorescent compound. Also added is 10-100 ppm of color shifter to better match the wavelength response of photomultiplier tubes (PMT). Stilbene crystal has superior neutron and gamma-ray PSD properties but they are more difficult to manufacture.

The mechanism for distinguishing neutrons from gamma rays using PSD is the difference in light output decay time for electron and proton excitations. Figure 9 shows the light output time dependence for gamma rays, fast neutrons, and alpha particles in a stilbene crystal detector. The NE-213 type liquid scintillators produce similar curves.

Data Acquisition System

Many PSD techniques have been developed. The one used here involves two constant-fraction discriminators (CFDs) to produce a zero-crossing pulse at 10% and 90% of the amplified signal. A delay-line amplifier is used to produce a rectangular amplified signal from the PMT, which is then sent to the CFDs. This signal has a fast rise and fall time and a rapid return to baseline. This provides excellent timing capabilities for the zero-crossing technique. The delay-line amplifier used here is an Ortec 460. A start and stop CFD trigger are created in the Ortec 552 Pulse-Shape Analyzer/Timing SCA. The start and stop triggers are then converted to an amplitude pulse in the

Ortec 567 TAC/SCA. The TAC signal and the energy signal are then sent to a FAST Comtec multiparameter data acquisition ADC for energy and TAC coincidence measurement and histogramming. This results in a two-dimensional histogram as shown in Figure 1.

The data acquisition system consists of a FAST Comtec four-channel multiparameter ADC, a coincidence interface module, and a PCI computer control card. The energy and TAC signals from the pulse processing electronics are fed to channel 1 and channel 2 of the ADC. If these signals are coincident within a preset window (currently 3.5 μs), a histogram pixel is incremented by one count in the two-dimensional histogram. Color gradients are used to indicate the number of counts at each pixel. Software allows a region-of-interest (ROI) to be drawn around the well separated fast neutrons.

Experimental Results

In addition to the interrogation of depleted uranium containing 80g 235U described above, we interrogated a 470g sample of HEU oxide embedded in a pallet of plywood. Data in this case was also taken with a single 3"x3" EJ-301 liquid scintillator detector (~1% solid angle). In both cases, the presence of the ^{235}U could be detected in only a few minutes with a relatively low flux of neutrons (~ 5 x 10^6 neutrons/sec). These experiments were conducted in different facilities, so in addition to the successful demonstration of the technique, we have also shown that the system is portable.

The plywood experimental setup is shown in Figure 10. Measurements were done with and without a 4 ft. x 8 ft. x 8 ft. pallet of plywood. The 470 g sample of HEU oxide (^{235}U mass ~376g) was placed on the center line of the pallet, 4 ft. up and 1 ft. from the end of the pallet. With the plywood present, the RFQ 60 keV neutron generator and detector were placed so that interrogating neutrons traveled through 2 ft. of plywood. The detected fission neutrons traveled through 1' of plywood.

The results of the measurements are summarized in Figure 11. Each of the measurements was 15 minutes. As can be seen, the measurements with beam on and HEU are 3-4σ above the measurements with beam on and no HEU. The measurements with beam on and HEU are 5-6σ above the measurements with beam off and no HEU.

This experiment was also simulated using MCNP5. The model used plywood (48 % hydrogen, 31 % carbon, and 21 % oxygen) with a density of 0.55 g/cm^3. The fast neutron detector model consisted of a right-circular cylinder (R=3.8 cm, L=7.6 cm) filled with a xylene-based liquid scintillator (NE-213), and surrounded by 5 cm of lead shielding on each side except the front. The simulation was done in two stages. First, the induced fission yield was determined to be 2.5×10^{-4} fission neutrons per source neutron. Second, fission neutrons were sourced isotropically and with a uniform spatial distribution within the HEU volume. The uranium was replaced with lead (Pb) in the simulation as a control case. The energy distribution of the fission neutrons was modeled as a Maxwellian spectrum with a temperature of 1.3 MeV.

For a neutron energy threshold of 1.5 MeV, this gives ~1 x 10^3 counts/40 billion source neutrons or 2.5 x 10^{-8} detected neutrons per source neutron. From the experimental data above, ~90 neutron counts >1.5 MeV were acquired in 15 minutes. The background rate with RFQ on and

no HEU is ~45 neutron counts. The counts above background then corresponds to ~1 x 10^{-8} detected neutrons per source neutron. This is in reasonable agreement with the MCNP results.

Conclusions

We have demonstrated a shielded-HEU detection technique that produces a clear positive signal in the presence of small quantities of ^{235}U. The technique uses a forward-directed, low-dose beam of 60 keV neutrons to induce ^{235}U fission when it is present. The induced fission produces fast neutrons which are then detected as the signature for the presence of ^{235}U. Interrogation of non-hydrogenous commerce by 60 keV neutrons offers the best SNM detection sensitivity per applied dose of any technique by several orders of magnitude. The ability to observe high-energy neutron emission while interrogating with low energy neutrons is a powerful and direct signature of SNM.

We envision an integrated system for a cargo scanning facility. This system will employ low-dose 60 keV neutron interrogation, low-dose radiography for hydrogenous cargo, and passive neutron and gamma-ray detection to inspect the full range of possible cargo, with minimal radiation exposure for personnel and minimal activation of surrounding materials. Such a system can efficiently and reliably clear commerce without undue delays.

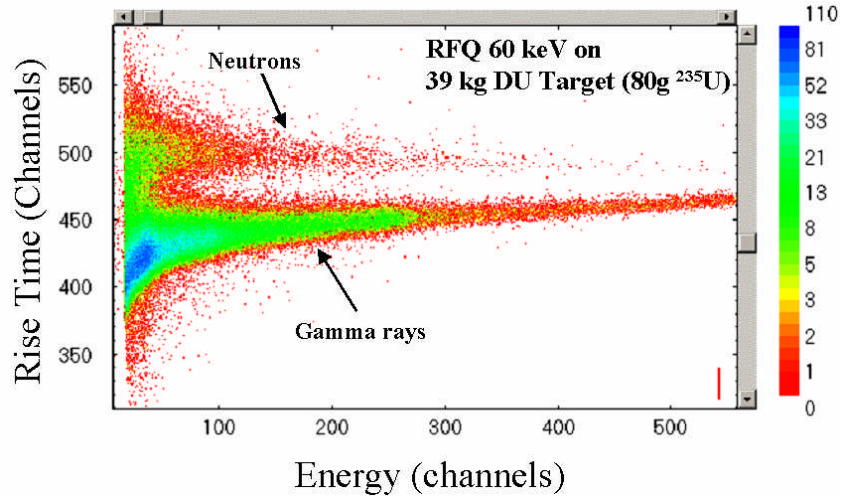

Figure 1 Two dimensional pulse-shape discrimination histogram obtained from a single 3"x3" liquid scintillator detector during 60-keV neutron interrogation of 80g of ^{235}U (39 kg depleted uranium). Notice the clear presence of an induced fission neutron band.

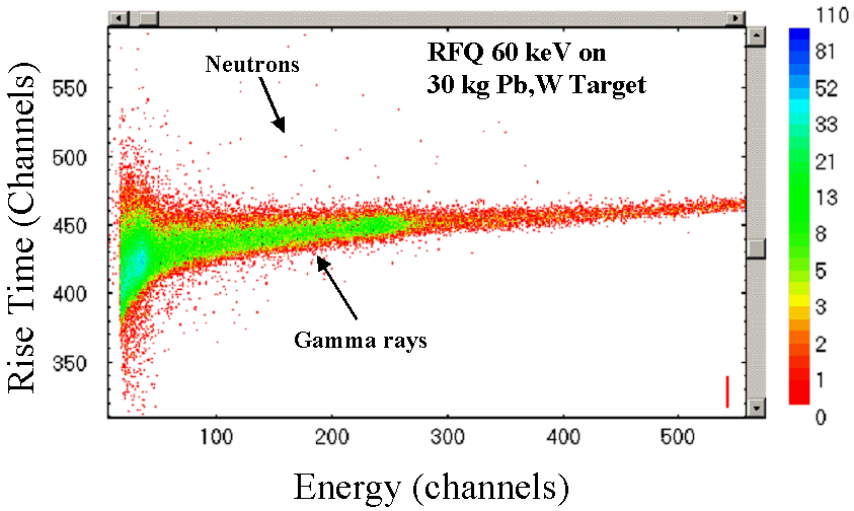

Figure 2 Two dimensional pulse-shape discrimination histogram obtained from a single 3"x3" liquid scintillator detector during 60-keV neutron interrogation of 30 kg of metal containing no ^{235}U. Notice the clear absence of an induced fission neutron band.

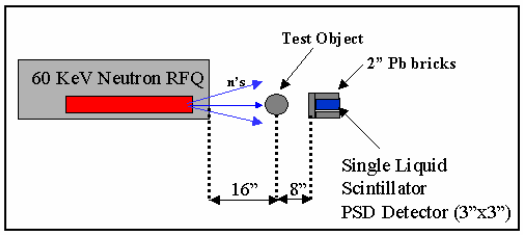

Figure 3 Experimental layout of 60-keV neutron interrogation of 80g ^{235}U (39 kg depleted uranium).

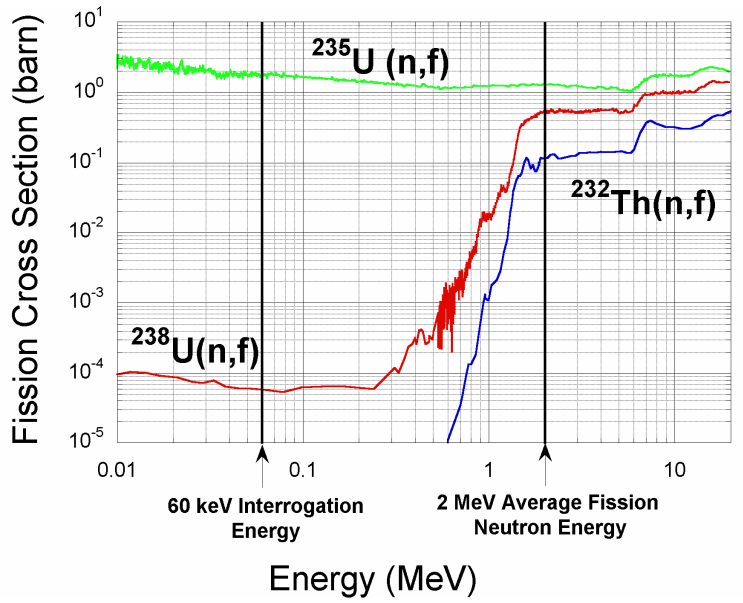

Figure 4 Neutron induced fission cross sections for ^{235}U, ^{238}U, and ^{232}Th. At 60 keV, the ^{238}U fission cross section is more than 4 orders of magnitude smaller than for ^{235}U, and the ^{232}Th fission cross section is orders of magnitude smaller still.

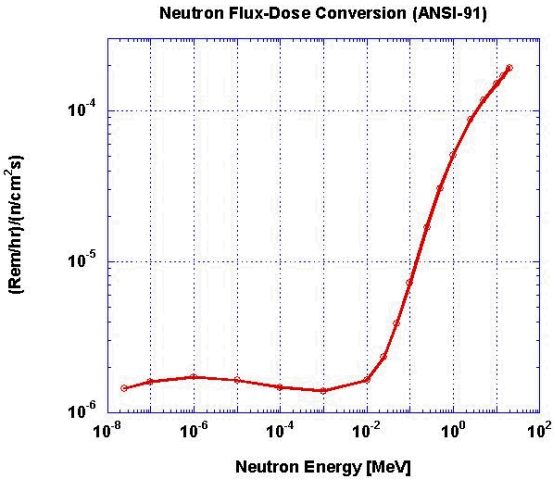

Figure 5 Neutron flux to dose (REM/hr)/(n/s/cm^2) conversion (ANSI-91) as a function of neutron energy.

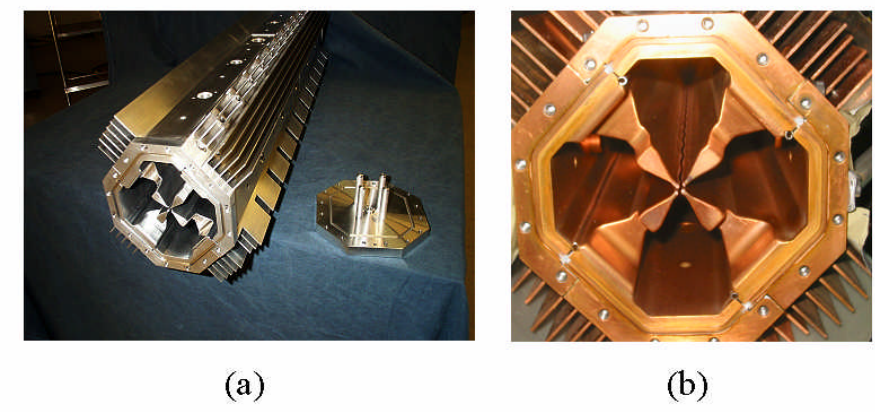

Figure 6 Photograph of the radio-frequency quadrupole cavity and four vane tips (a), and a close up photograph of the vane tips (b).

Figure 7 Photograph of fully assembled portable RFQ 60 keV neutron generator

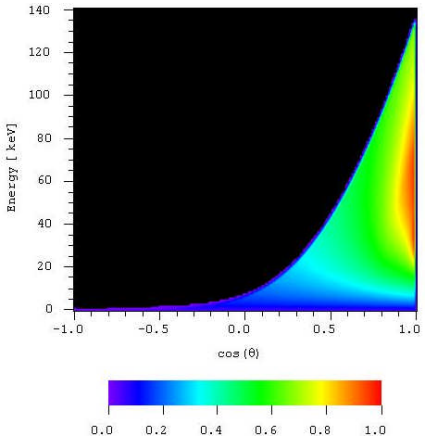

Figure 8 Calculated neutron beam profile distribution of energy and intensity as a function of angle away from the beam axis for the ^{7}Li(p,n) reaction. The incident proton energy is 1.93 MeV.

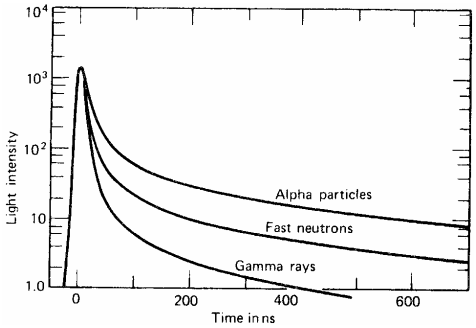

Figure 9 Time dependence of scintillation pulses in stilbene when excited by different incident particle types [1].

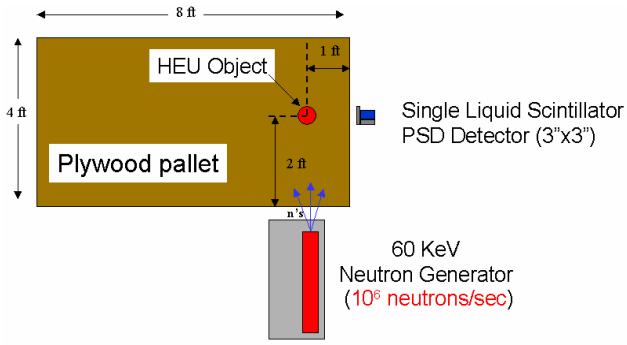

Figure 10 Diagram of the experimental setup with HEU embedded in Plywood.

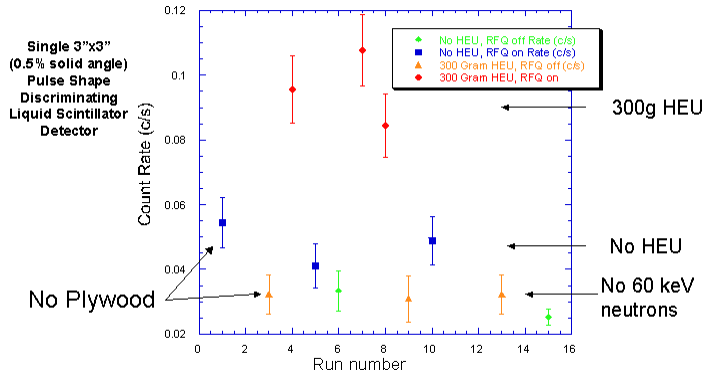

Figure 11 Count rates for the 60 keV neutron interrogation of 470g of HEU oxide in Plywood. All measurements were 15 minutes in duration and obtained with a single 3"x3" EJ-301 liquid scintillator detector.

Table 1 MCNP Simulation of Fission Probability per Source Neutron for Various Materials

	Cargo			
Source	**Water**	**Aluminum (Al)**	**Iron (Fe)**	**Lead (Pb)**
60 keV (directional)	3.9e-8	3.9e-4	4.3e-4	4.6e-4
2.5 MeV (isotropic)	9.3e-7	9.5e-5	6.9e-5	6.6e-5
7 MeV (isotropic)	1.3e-5	9.4e-5	7.6e-5	7.5e-5
14.1 MeV (isotropic)	3.2e-5	9.6e-5	1.0e-4	1.2e-4

[1] L. M. Bollinger and G. E. Thomas, Reviews of Scientific Instruments 32, 1044 (1961).

[2] Passive Nondestructive Assay of Nuclear Materials, Doug Reilly, Norbert Ensslin, Hastings Smith, Jr., and Sarah Kreiner, editors; 1991, LA-UR-90-732.

This work was performed under the auspices of the U. S. Department of Energy by University of California, Lawrence Livermore National Laboratory under contract W-7405-Eng-48.